

Influence of dispersion on the resonant interaction between three incoherent waves

Antonio Picozzi^{1,2} and Pierre Aschieri¹¹*CNRS-LPMC, Université de Nice Sophia-Antipolis, Nice, France*²*Laboratoire de Physique de l'Université de Bourgogne, CNRS, Dijon, France*

(Received 13 June 2005; published 13 October 2005)

We study the influence of group-velocity dispersion (or diffraction) on the coherence properties of the parametric three-wave interaction driven from an incoherent pump wave. We show that, under certain conditions, the incoherent pump may efficiently amplify a signal wave with a high degree of coherence, in contrast with the usual kinetic description of the incoherent three-wave interaction. The group-velocity dispersion is shown to be responsible for a spectral filtering process, in which the coherence of the generated signal increases, as the coherence of the pump wave decreases. As a result, the coherence acquired by the signal in the presence of an incoherent pump, is higher than that acquired in the presence of a fully coherent pump. The mechanism underlying this intriguing result is based on the emergence of a mutual coherence between the incoherent pump and the generated idler wave. We calculate explicitly the degree of mutual coherence between the pump and idler waves and show that the two incoherent waves become completely correlated in the full incoherent regime of interaction. The theory is in quantitative agreement with the numerical simulations. To motivate the experimental confirmation of our theory, we characterize the dispersion properties of an actual quadratic nonlinear optical crystal in which the process of signal coherence enhancement induced by pump incoherence may be studied experimentally.

DOI: [10.1103/PhysRevE.72.046606](https://doi.org/10.1103/PhysRevE.72.046606)

PACS number(s): 42.65.Sf, 42.65.Yj, 42.25.Kb

I. INTRODUCTION

Resonant wave interactions take place in any dispersive and weakly nonlinear medium whose lowest order is quadratic or cubic in terms of the waves amplitudes [1,2]. For this reason they play a fundamental role in physics and are thus found in such diverse fields as hydrodynamics [3], nonlinear acoustics [4], plasma [5–7], nonlinear optics [8–10], and matter waves [11].

In the present work we consider the parametric three-wave interaction, which is among the most largely studied configuration of resonant wave interactions. It refers to a parametric amplification process where energy is transferred from a high frequency wave (pump) towards two waves of lower frequencies, which are usually called the signal and the idler waves in the context of nonlinear optics. From the theoretical point of view, two alternative approaches are usually employed to describe the three-wave parametric interaction [5–7,12,13]. On the one hand, when the time correlation τ_c of the pump wave is much larger than the characteristic time τ_0 of nonlinear interaction, i.e., $\tau_c \gg \tau_0$, one usually finds the coherent phase approximation. In this coherent regime of interaction the relation between the phases of the three waves is significant to the description of their interaction. The equations governing this coherent evolution of the fields have been studied in various physical contexts. In particular, soliton solutions have been identified in the presence of convection (group-velocity difference) [14,15], or dispersion (group-velocity dispersion) [9,10,16,17]. On the other hand, when the time correlation of the pump wave becomes much smaller than the nonlinear interaction time, $\tau_c \ll \tau_0$, one usually applies the random phase approximation. In this approach, the three waves are implicitly assumed to be incoherent, so that their relative phases are no longer significant to their interaction. Phase information is thus averaged out,

to obtain a weak-turbulence description of the interaction in terms of irreversible kinetic equations. This kinetic approach of the three-wave interaction has been widely investigated in plasma physics, especially as regards the important issue of inertial confinement fusion [18].

The coherent and incoherent regimes of three-wave interaction are commonly considered as being well distinct. This has been confirmed in a recent work, where the transition between the two regimes is shown to occur suddenly as the time correlation τ_c of the pump wave is varied [12]. However, this work was based on a rather simple three-wave model that neglected the influence of dispersion on wave propagation. Conversely, linear dispersive effects have been shown to affect considerably the properties of coherence of the waves during their nonlinear evolution [19–24]. In particular, the analysis of (group-velocity) dispersion on the degenerate configuration of the three-wave interaction revealed the existence of a peculiar condensation process [24]. It consists of a sudden transition of coherence, in which the incoherent pump and incoherent signal waves, spontaneously evolve towards a coherent state. During this transition, the energy of the incoherent waves concentrates in the vicinity of the signal and pump carrier wave frequencies. As a result, the condensation process is characterized by a spontaneous evolution of the system from the fully incoherent regime ($\tau_c \ll \tau_0$) towards the coherent regime ($\tau_c \gg \tau_0$) of interaction.

The present work is devoted to the study of this transition of coherence in the general framework of the nondegenerate configuration of the three-wave interaction. It is shown that, contrary to the degenerate case where both waves evolve towards a coherent state [24], in the nondegenerate case the system may evolve towards a mixed regime of interaction. This mixed regime is characterized by the coexistence of two incoherent waves, the pump and the idler, together with a

coherent signal wave. More precisely, we show that the existence of the mixed regime of interaction relies on the emergence of a mutual coherence between the incoherent pump and the incoherent idler wave, so that their random phases result to be locked with each other. In this way, the idler wave may “absorb” the fluctuations of the incoherent pump, which in turn allows the signal to evolve towards a highly coherent state.

A similar mixed regime of coherent-incoherent interaction was shown to be induced by the group-velocity difference, i.e., convection, between the three waves [20,21]. In particular, it was shown that the convection-induced phase-locking mechanism was responsible for the generation of incoherent solitons [20], that were subsequently observed experimentally in cubic nonlinear media [23]. Let us mention that this particular mixed interaction regime was also studied experimentally in quadratic nonlinear media by exploiting the specific phase-matching conditions inherent to conical optical beams [25].

In these previous studies [19–21,23], the phase-locking mechanism was induced by the convection between the three waves, whereas in the present work the phase locking is shown to result solely from the (group-velocity) dispersion. Actually, dispersion is responsible for a remarkable dynamical feature that does not occur through convection. We show that group-velocity dispersion leads to an intriguing spectral filtering process, in which the coherence of the generated signal wave increases, as the coherence of the pump wave decreases. More precisely, the coherence acquired by the signal in the presence of an incoherent pump, is higher than that acquired in the presence of a fully coherent pump. This counterintuitive result is in strong contradiction with the kinetic theory and the random-phase approximation approach, which are supposed to be more accurate as the incoherence of the pump wave is increased.

To motivate the experimental confirmation of our theory, we present our work in the context of nonlinear optics, because quadratic nonlinear media offer unique opportunities for the experimental study of the parametric generation process. In particular, we characterize the dispersion properties of an actual quadratic nonlinear crystal in which the process of signal coherence enhancement induced by pump incoherence may be studied experimentally.

II. GOVERNING EQUATIONS

To describe the spatio-temporal evolution of the fields in a quadratic nonlinear medium, we consider the usual three-wave interaction equations in one spatial dimension. Let us assume that the spectral width of the three interacting waves are much smaller than their respective carrier frequencies ($\Delta\omega_j \ll \omega_j$, $j=1, 2, 3$ with $\omega_3 = \omega_1 + \omega_2$), so that the slowly varying envelope approximation is justified. The coupled partial differential equations governing the evolution of the amplitude envelopes A_j read

$$i \frac{\partial A_1}{\partial z} = \frac{\delta H}{\delta A_1^*} = -A_3 A_2^* - \beta_1 \frac{\partial^2 A_1}{\partial t^2} - i\rho_1 \frac{\partial A_1}{\partial t}, \quad (1)$$

$$i \frac{\partial A_2}{\partial z} = \frac{\delta H}{\delta A_2^*} = -A_3 A_1^* - \beta_2 \frac{\partial^2 A_2}{\partial t^2} - i\rho_2 \frac{\partial A_2}{\partial t}, \quad (2)$$

$$i \frac{\partial A_3}{\partial z} = \frac{\delta H}{\delta A_3^*} = -A_1 A_2 - \beta_3 \frac{\partial^2 A_3}{\partial t^2}, \quad (3)$$

where $H = \int \mathcal{H} dt$ is the field Hamiltonian, and \mathcal{H} its density. The Hamiltonian has a linear and a nonlinear contribution ($H = H_L + H_{NL}$), whose respective densities read

$$\mathcal{H}_L = \left(\frac{i}{2} \sum_{j=1}^2 \rho_j A_j \partial_t A_j^* + \text{c. c.} \right) + \sum_{j=1}^3 \beta_j |\partial_t A_j|^2, \quad (4)$$

$$\mathcal{H}_{NL} = -A_1 A_2 A_3^* - A_1^* A_2^* A_3. \quad (5)$$

For definiteness we call A_1, A_2, A_3 the signal, idler, and pump waves, respectively. Equations (1)–(3) are written in the reference frame of the pump wave, so that the dimensionless parameters $\rho_j = (v_3 - v_j)/v_j$ ($j=1, 2$) represent the amount of convection between the daughter waves $A_{1,2}$ and the pump wave A_3 , where v_j are the group velocities of the three waves ($j=1, 2, 3$). For convenience, we normalized the problem with respect to the characteristic nonlinear length $L_{nl} = 1/(\gamma e_0)$ and time $\tau_0 = L_{nl}/v_3$, where $e_0 = \langle |A_3|^2 \rangle^{1/2}$ is the average amplitude of the pump, the symbol $\langle \dots \rangle$ denotes a stochastic average over an ensemble of realizations with random initial conditions. The nonlinear coefficient γ is assumed to be identical for the three waves. The variables can be recovered in real units through the transformations $z \rightarrow z L_{nl}$; $t \rightarrow t \tau_0$ and $A_i \rightarrow A_i e_0$. With these units, the dimensionless dispersion coefficients read $\beta_j = k''_j v_3 / \tau_0$, $k''_j = (\partial^2 k / \partial \omega^2)_j$ being the dispersion parameter and $k(\omega)$ the wave vector modulus at frequency ω .

To determine the key parameters that govern the parametric amplification process, let us define the relevant characteristic lengths of the problem. The influence of pump dispersion is determined by the characteristic length $L_d = \tau_c^2 / |k''_3|$, where τ_c is the time correlation of the pump wave. The influence of convection between the pump A_3 and the daughter waves $A_{1,2}$ is characterized by the propagation lengths $L_{cv,j} = \tau_c / |1/v_j - 1/v_3|$ ($j=1, 2$). Defining the dimensionless parameter $\sigma = \tau_0 / \tau_c$, we have

$$\frac{L_d}{L_{nl}} = \frac{1}{\sigma^2 |\beta_3|}, \quad (6)$$

$$\frac{L_{cv,j}}{L_{nl}} = \frac{1}{\sigma |\rho_j|} \quad (j=1, 2). \quad (7)$$

These relations allow us to precise the criterion for applicability of the random phase approximation. When $L_d/L_{nl} \ll 1$, and $L_{cv,j}/L_{nl} \ll 1$ (i.e., $\varepsilon = H_{NL}/H_L \ll 1$), the rapid fluctuations of the incoherent pump make linear dispersive effects dominant with respect to nonlinear effects, and the random phase approximation approach is usually applied [2].

Let us note that Eqs. (1)–(3) also hold for the description of purely transverse spatial evolution of the three beams. Indeed, the substitution of dispersion with diffraction, and convection with beam walk-off, transforms Eqs. (1)–(3) into

the well-known equations describing purely transverse effects in quadratic nonlinear media [9,10,16,17].

III. COHERENT SIGNAL GENERATION FROM AN INCOHERENT PUMP

The role of convection (ρ_j) on the coherence properties of the three-wave interaction, especially as regards the phase-locking mechanism, was extensively investigated in Ref. [21]. Our purpose here is to study the influence of dispersion effects in the strongly incoherent regime of interaction $L_d/L_{nl} \ll 1$. We will show that, in marked contrast with the kinetic approach, the incoherent pump may lead to the generation of a highly coherent signal wave. In this section we adapt the theory developed in the degenerate case [24] to the nondegenerate configuration considered here. We calculate explicitly the dispersion relation (spectral gain curve) of the signal wave in the presence of an incoherent pump. We will see that the dispersion relation allows us to describe the essential properties of coherence of the parametric generation process in a general framework.

A. Dispersion relation of the signal wave

We consider the regime of parametric amplification where a high amplitude incoherent pump A_3 amplifies the daughter waves A_1 and A_2 from noise fluctuations. In this linear regime of interaction, the incoherent pump is assumed to be not affected by the daughter waves, $|A_3| \gg |A_{1,2}|$, so that Eq. (3) may be linearized and solved *via* a standard Fourier transform technique, $\tilde{A}_3(z, \omega) = \tilde{A}_{3,0}(\omega) \exp(-i\beta_3 \omega^2 z)$, where $\tilde{A}_{3,0}(\omega)$ is the Fourier transform of the pump amplitude $A_3(z=0, t)$ at the entry of the nonlinear medium. In the following we assume that the three fields obey a Gaussian statistics, which may be considered as a severe approximation considering the nonlinear character of the evolution of the fields. However, the assumption of Gaussian statistics is justified here because linear dispersive effects dominate nonlinear effects ($L_d/L_{nl} \ll 1$) [2]. We also assume that the pump wave is of zero mean $\langle A_3(z, t) \rangle = \langle \tilde{A}_3(z, \omega) \rangle = \langle \tilde{A}_{3,0}(\omega) \rangle = 0$, and statistically stationary (translational invariant), so that its spectrum is δ -correlated $\langle \tilde{A}_{3,0}(\omega + \omega') \tilde{A}_{3,0}^*(\omega) \rangle = (2\pi)^2 \Gamma(\omega) \delta(\omega')$, $\Gamma(\omega)$ representing the pump spectral density [26]. Under these conditions, Eqs. (1) and (2) may be linearized and solved by means of the Fourier expansion. The formal solution to Eq. (2) gives the evolution of the idler wave

$$\begin{aligned} \tilde{A}_2(z, \omega) &= \frac{i}{(2\pi)^2} \int_0^z dz' \int_{-\infty}^{\infty} d\omega_1 \exp[-i(\beta_2 \omega^2 + \rho_2 \omega)(z - z')] \\ &\quad \times \tilde{A}_{3,0}(\omega_1) \tilde{A}_1^*(z', \omega_1 - \omega) \exp(-i\beta_3 \omega_1^2 z'). \end{aligned}$$

This expression may be substituted in Eq. (1) to get a closed equation for the evolution of the signal wave, in terms of the incoherent pump amplitude,

$$\begin{aligned} \partial_z \tilde{A}_1 + i(\rho_1 \omega + \beta_1 \omega^2) \tilde{A}_1 &= \int \int_{\mathcal{R}^2} d\omega_1 d\omega_2 \int_0^z dz' \frac{\exp(i\phi)}{(2\pi)^2} \\ &\quad \times \tilde{A}_1(z', \omega + \omega_2 - \omega_1) \tilde{A}_{3,0}(\omega_1) \tilde{A}_{3,0}^*(\omega_2), \end{aligned} \quad (8)$$

where $\phi = [\rho_2(\omega_1 - \omega) + \beta_2(\omega_1 - \omega)^2](z - z') + \beta_3(\omega_2^2 z' - \omega_1^2 z)$. Let us now take an average of this equation over the ensemble of realizations. The third order correlator in Eq. (8) can be factorized as

$$\begin{aligned} \langle \tilde{A}_1(z', \omega + \omega_2 - \omega_1) \tilde{A}_{3,0}(\omega_1) \tilde{A}_{3,0}^*(\omega_2) \rangle &= \langle \tilde{A}_1(z', \omega + \omega_2 - \omega_1) \rangle \langle \tilde{A}_{3,0}(\omega_1) \tilde{A}_{3,0}^*(\omega_2) \rangle \end{aligned} \quad (9)$$

by virtue of the factorizability property of statistical Gaussian fields [26].

Let us remark that the factorization (9) is significant because we are looking for the generation of a coherent signal wave. We thus assume that the signal and the pump fields are not correlated, and, more importantly, we assume that the average of the signal wave does not vanish, $\langle \tilde{A}_1(z, \omega) \rangle \neq 0$. Accordingly, a first order perturbation theory in $\varepsilon = H_{NL}/H_L \ll 1$ [see Eqs. (6) and (7)] may be used to get a closed equation for the evolution of the average of the signal wave. This contrasts with the usual random phase approximation approach, where the fields are implicitly assumed to be incoherent (random phase fields), so that their average amplitudes are assumed to vanish, $\langle \tilde{A}_j(z, \omega) \rangle = 0$ ($j=1, 2, 3$) [2,5,6,13]. It turns out that a first order perturbation theory is no longer sufficient to achieve a closure of the moments' equations, and one must resort to a second order approximation in $\varepsilon = H_{NL}/H_L$ [2].

Using the factorization (9) and Eq. (8), one obtains an equation governing the evolution of the averaged signal in terms of the incoherent pump spectrum $\Gamma(\omega)$. By means of the Laplace transform, $\langle \hat{A}_1(\lambda, \omega) \rangle = \int_0^\infty \langle \tilde{A}_1(z, \omega) \rangle \exp(-\lambda z) dz$, one may then derive the dispersion relation of the signal in the presence of the incoherent pump,

$$\lambda + i\beta_1 \omega^2 + i\rho_1 \omega = \int_{-\infty}^{+\infty} \frac{\Gamma(x)}{D_\lambda(x)} dx, \quad (10)$$

where

$$D_\lambda(x) = \lambda + i\beta_3 x^2 - i\beta_2(x - \omega)^2 - i\rho_2(x - \omega). \quad (11)$$

We pursue the analytical study by assuming that the initial pump spectrum has a Lorentzian shape, $\Gamma(\omega) = (\sigma/\pi)/(\sigma^2 + \omega^2)$, where $\sigma = \tau_0/\tau_c$ [see Eqs. (6) and (7)] represents the normalized spectral width of $\Gamma(\omega)$, which characterizes the degree of coherence of the pump wave. The explicit dispersion relation $\lambda(\omega)$ cannot be derived from Eqs. (10) and (11) in the general case. However, to get an insight into the coherence properties of the signal wave, let us study the growth rate of its homogenous mode $\omega=0$ in the velocity matched case $\rho_j=0$ ($j=1, 2$). In this limit, the integrand of Eq. (10) has four poles located at $x_1^\pm = \pm i\sigma$ and $x_2^\pm = \pm \sqrt{i\lambda/(\beta_3 - \beta_2)}$, so that integral (10) can be readily calcu-

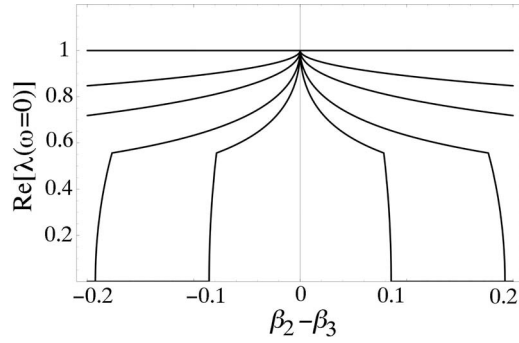


FIG. 1. Growth rate of the homogenous signal mode $\omega=0$ as a function of the mismatch of the dispersion parameters of the idler and pump waves, $\epsilon=\beta_2-\beta_3$. If $\beta_2=\beta_3$, the homogenous signal mode is efficiently amplified $\text{Re}[\lambda(\omega=0)]=1$ regardless of the degree of pump incoherence σ . From the upper to the bottom curve, $\sigma=0, \sigma=1, \sigma=2, \sigma=4, \sigma=6$.

lated by the method of residues, yielding $\lambda[\lambda(\lambda+i\epsilon\sigma^2)-1]^2 = -i\epsilon\sigma^2$, where $\epsilon=\beta_2-\beta_3$. Figure 1 illustrates the physical relevant solution for different values of σ . For $\sigma=0$, i.e., $\Gamma(\omega)=\delta(\omega)$, we recover the trivial solution $\text{Re}(\lambda)=1$ of the coherent problem, the homogenous mode $\omega=0$ of the signal wave is amplified with the maximum growth rate, whatever the values of the dispersion parameters of the pump and idler waves (β_2, β_3). The unexpected result is that the homogenous signal mode may be amplified by the incoherent pump ($\sigma \neq 0$) with the same growth rate [$\text{Re}(\lambda)=1$], provided that the dispersion coefficients of the pump and idler waves coincide ($\beta_2=\beta_3$). Note that this efficient amplification of the homogenous signal mode occurs whatever the value of its dispersion parameter β_1 .

We clarified this result by calculating the spectral gain profile $\text{Re}[\lambda(\omega)]$ for any ω , in the limit $\beta_2=\beta_3$. For this purpose, we remark that one of the four poles of the integrand (10) tends to infinity as β_2 tends to β_3 , so that its contribution to the integral vanishes in this limit. The three permanent poles allow us to explicitly calculate the dispersion relation of the signal wave in the limit $\beta_2=\beta_3$,

$$\lambda = i \frac{\beta_2 - \beta_1}{2} \omega^2 - s \beta_2 \omega \sigma + s \frac{\sigma \rho_2}{2} - i \frac{\rho_1 + \rho_2}{2} \omega + \sqrt{Q}, \quad (12)$$

where

$$Q = 1 - \frac{1}{4} [\rho_1 \omega + 2i\beta_2 \omega s \sigma - \rho_2(\omega + i s \sigma) + (\beta_1 + \beta_2) \omega^2]^2$$

and $s = \text{sign}(2\beta_2\omega - \rho_2)$.

The dispersion relation (12) extends to the nondegenerate configuration of the parametric interaction the dispersion relation obtained in Ref. [24] for the degenerate case ($A_1=A_2$). Indeed, by setting $\rho_1=\rho_2, \beta_1=\beta_2$, Eq. (12) recovers the dispersion relation obtained in Ref. [24]. This means that the condensation process reported in Ref. [24] may also occur in the nondegenerate configuration provided that the dispersion parameters of the three waves are matched ($\beta_1=\beta_2=\beta_3$). In that case the initially incoherent three waves evolve towards a coherent regime of interaction, a feature

that we have confirmed by numerical integration of Eqs. (1)–(3). However, the conditions required to simultaneously match the dispersion parameters of the three waves in a realistic experiment are quite artificial, so that we have not deepened the properties of this three-wave condensation process.

B. Analysis of the dispersion relation

Before discussing the influence of group-velocity dispersion on the coherence properties of the signal wave, it is interesting to observe that Eq. (12) allows us to describe the main characteristic features of the parametric generation process in a general framework. Let us thus study the dispersion relation (12) in various different limits of interest.

1. Coherent pump limit

First of all, let us consider the limit of coherent excitation, where the pump A_3 is assumed to be a continuous wave [$\Gamma = \delta(\omega), \sigma=0$]. In this limit we recover the spectral gain curve of the full coherent problem (see, e.g., Refs. [27,28])

$$\text{Re}[\lambda(\omega)] = \sqrt{1 - [(\beta_1 + \beta_2)\omega^2 + (\rho_1 - \rho_2)\omega]^2/4}. \quad (13)$$

It is apparent from Eq. (13) that $\text{Re}[\lambda(\omega)]$ exhibits a maximum at $\omega=0$, so that the homogenous signal mode is preferentially amplified by the coherent pump wave. Let us remark that the gain curve induced by dispersion [Eq. (13) with $\rho_{1,2}=0$] displays a flatter peak at $\omega=0$ as compared to that induced by convection [Eq. (13) with $\beta_{1,2}=0$]. This simply means that the selection of the homogenous mode is more efficient when the parametric process is ruled by convection rather than dispersion. These aspects have been extensively investigated in the literature [27,28]. Also note that in the degenerate configuration ($A_1=A_2, \beta_1=\beta_2$, and $\rho_1=\rho_2$), Eq. (13) reduces to $\text{Re}[\lambda(\omega)] = \sqrt{1 - \beta_1^2 \omega^4}$, which is the well-known gain curve of the degenerate parametric amplification process.

2. Role of convection

It is interesting to observe that the role of convection on the coherence of the signal wave may also be described by the dispersion relation (12). Indeed, in the dispersionless limit ($\beta_j=0$), the spectral gain curve (12) reduces to

$$\lambda(\omega) = -\sigma \frac{|\rho_2|}{2} + \sqrt{1 - \frac{1}{4} [(\rho_1 - \rho_2)\omega + i\sigma\rho_2]^2}, \quad (14)$$

where we have omitted the purely imaginary term $i(\rho_1 + \rho_2)\omega/2$ that does not contribute to the growth rate $\text{Re}[\lambda(\omega)]$. Two physical interesting limits of Eq. (14) deserve to be commented.

(i) $\rho_1=\rho_2$: This case is relevant for the description of the degenerate configuration of the parametric amplification process ($A_1=A_2$). The spectral gain curve (14) then reduces to

$$\text{Re}(\lambda) = -\sigma|\rho_1|/2 + \sqrt{1 + \sigma^2\rho_1^2/4}. \quad (15)$$

In this limit the gain curve becomes completely flat, since $\text{Re}(\lambda)$ in (15) does not depend on ω . This means that no

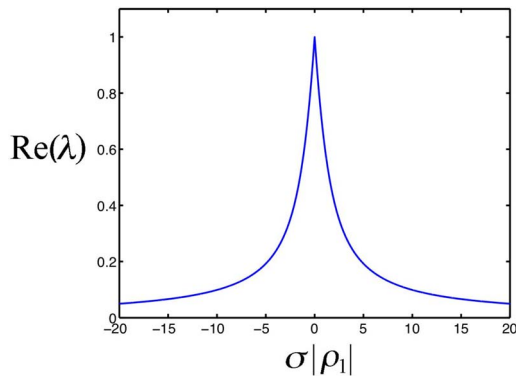


FIG. 2. (Color online) Influence of convection (group-velocity difference) on the signal growth rate in the degenerate configuration of the parametric amplification process [from Eq. (15)]. When $\sigma|\rho_1| \gg 1$ ($L_{nl} \gg L_{cv}$) the amplification of the signal is quenched by the incoherent pump. Conversely, when $\sigma|\rho_1| \ll 1$, the regime of interaction is coherent, i.e., $L_{nl} \ll L_{cv}$, and the signal may be efficiently amplified.

coherence enhancement may occur for the signal wave, regardless of the degree of coherence of the pump (σ). Nevertheless, the incoherent signal wave may be efficiently amplified when $\sigma|\rho_1| \ll 1$, as revealed by Fig. 2, that illustrates the gain curve $\text{Re}(\lambda)$ vs $\sigma|\rho_1|$ [Eq. (15)]. Indeed, when $\sigma|\rho_1| \ll 1$, nonlinear effects dominate linear convective effects [$L_{nl} \ll L_{cv}$ from Eq. (7)]. This means that the random fluctuations of the pump are too slow to influence the evolution of the signal wave, which can thus be efficiently amplified during the propagation, as if the pump were almost coherent. Conversely, in the limit $\sigma|\rho_1| \gg 1$ ($L_{nl} \gg L_{cv}$), pump fluctuations are shown to quench the amplification of the signal wave, whose parametric growth-rate $\text{Re}(\lambda)$ tends to zero (Fig. 2). These properties of coherence of the degenerate parametric amplification process were obtained in Ref. [21] from a completely different, and rather involved, theoretical approach.

(ii) Another interesting limit of Eq. (14) is $\rho_2=0$, i.e., the limit in which the velocities of the pump and idler waves are matched. In this case the gain curve (14) reduces to

$$\text{Re}(\lambda) = \sqrt{1 - \omega^2 \rho_1^2 / 4}. \quad (16)$$

Let us emphasize that in this limit, the gain curve of the signal does not depend on the degree of coherence of the pump σ , which means that, regardless of pump incoherence, the signal may be efficiently generated. More precisely, the gain curve (16) coincides with that obtained in the full coherent problem [see Eq. (13) for $\rho_2 = \beta_{1,2} = 0$]. Indeed, it has been shown in Refs. [20,21] that when the velocities of the idler and pump waves are matched ($\rho_2=0$), the signal may be efficiently amplified with a high degree of coherence, as if the pump were fully coherent. This may occur owing to a convection-induced phase-locking mechanism between the pump and idler waves. We refer the reader to Ref. [21] for an extensive discussion of this mixed regime of coherent-incoherent interaction induced by convection.

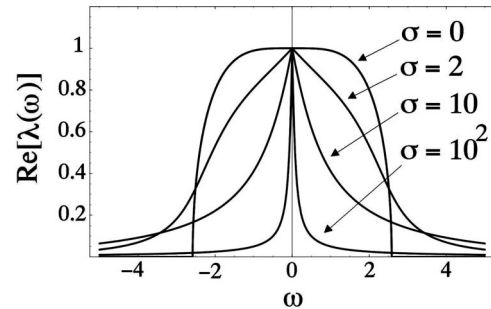


FIG. 3. Spectral gain curve of the signal wave obtained from Eq. (17), for different values of the degree of coherence of the pump wave σ . The coherence of the generated signal increases as the coherence of the pump decreases. Dispersion parameters are $\beta_1=0.2, \beta_2=\beta_3=0.1$.

3. Role of dispersion

Let us now analyze the role of dispersion on the spectral gain curve of the signal wave. For this purpose, let us neglect the influence of convection on the parametric instability (i.e., $L_{cv} \gg L_{nl}, L_{cv} \gg L_d$), so that Eq. (12) with $\rho_1 = \rho_2 = 0$ reduces to

$$\lambda(\omega) = -|\beta_2 \omega| \sigma + \sqrt{1 - [(\beta_1 + \beta_2) \omega^2 + 2i|\beta_2 \omega| \sigma]^2 / 4}, \quad (17)$$

where we have omitted the irrelevant purely imaginary term $i(\beta_2 - \beta_1) \omega^2 / 2$, that does not affect the gain curve $\text{Re}[\lambda(\omega)]$. Figure 3 shows the spectral gain curve (17) for different values of the degree of coherence of the pump wave. For $\sigma=0$, Eq. (17) recovers the gain curve in the limit of coherent excitation [see Eq. (13) for $\rho_{1,2}=0$]. The surprising result is that the spectral gain curve becomes narrower as the coherence of the pump is degraded, which entails a preferential amplification of the homogenous signal mode $\omega=0$. This means that the fluctuations of the pump appear as having a filtering action on the signal spectrum, which thus unexpectedly favor the generation of a coherent signal. Note in Fig. 3 that the spectral gain curve of the coherent problem ($\sigma=0$) exhibits a frequency cutoff, $\lambda(\omega)=0$ for $|\omega| \geq \omega_c = \sqrt{2/|\beta_1 + \beta_2|}$. Interestingly, this frequency cutoff is removed under incoherent excitation $\sigma \neq 0$, so that the preferential amplification of the homogenous signal mode $\omega=0$ is accompanied by a weak growing of higher frequencies.

The process of spectral filtering induced by pump incoherence has been verified by numerical integration of Eq. (1). A very good agreement has been obtained between expression (17) and the simulations. Figure 4 shows the signal spectra generated from an incoherent pump [Fig. 4(a)] and a fully coherent pump [Fig. 4(c)]. Figures 4(b)–4(d) show the respective spectra of the idler wave. Under coherent excitation ($\sigma=0$), the degree of coherence of the signal and idler waves are the same [Figs. 4(c) and 4(d)]. Conversely, when the parametric interaction is driven from an incoherent pump, the generation of the highly coherent signal takes place at the detriment of the amplification of an incoherent idler wave [Fig. 4(b)]. In the next section we will see that the

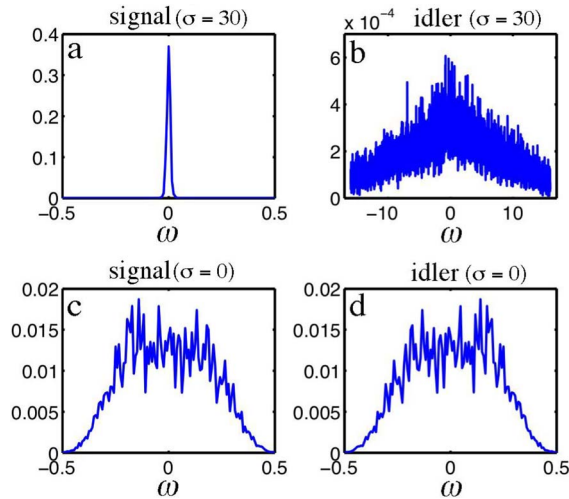


FIG. 4. (Color online) Numerical simulations of Eqs. (1)–(3) confirming the process of signal coherence enhancement induced by pump incoherence predicted through Eq. (17) (see Fig. 3). Spectrum of the signal wave at the propagation distance $z=10$, when it is generated from an incoherent pump [(a) $\sigma=30$], and a fully coherent pump [(c) $\sigma=0$]. (b)–(d) show the respective idler spectra [(b) $\sigma=30$, (d) $\sigma=0$]. Let us remark that the signal and idler spectra generated from a coherent pump are almost phase conjugated with each other. Note the change of the limits of the frequency window in (b). An average over 20 numerical simulations has been taken ($\beta_1=0.2, \beta_2=\beta_3=0.1$).

idler spectrum actually evolves towards the spectrum of the incoherent pump wave.

Let us finally remark that the spectral filtering process induced by dispersion persists in the presence of convection between the interacting waves. This is clearly illustrated in Fig. 5(a), that shows the theoretical spectral gain curve [Eq. (12)] under coherent ($\sigma=0$) and incoherent ($\sigma \neq 0$) excitation in the presence of convection. The unexpected result is that convection leads to a significant spectral shift of the amplified signal wave. This result is confirmed by the numerical simulations of Eqs. (1)–(3), as shown in Fig. 5(b), that illustrates the averaged signal spectrum at the propagation distance $z=10$. Note that the signal spectrum in (b) is well approximated by $\langle |\tilde{A}_1|^2(z_0, \omega) \rangle \propto \exp\{2 \operatorname{Re}[\lambda(\omega)]z_0\}$, confirming the good agreement between Eq. (12) and the simulations. The spectral shift of the amplified signal wave is remarkable because it originates in the noise fluctuations of the pump wave *via* the combined effects of dispersion and convection. This noise-induced spectral shift is expected to occur in any realistic experimental configuration, as will be discussed in Sec. V.

IV. PUMP-IDLER PHASE-LOCKING INDUCED BY DISPERSION

In the preceding section we have shown that, owing to group-velocity dispersion, the coherence acquired by the signal wave may increase, as the coherence of the pump wave decreases. A similar phenomenon of coherence enhancement induced by pump incoherence has recently been reported in

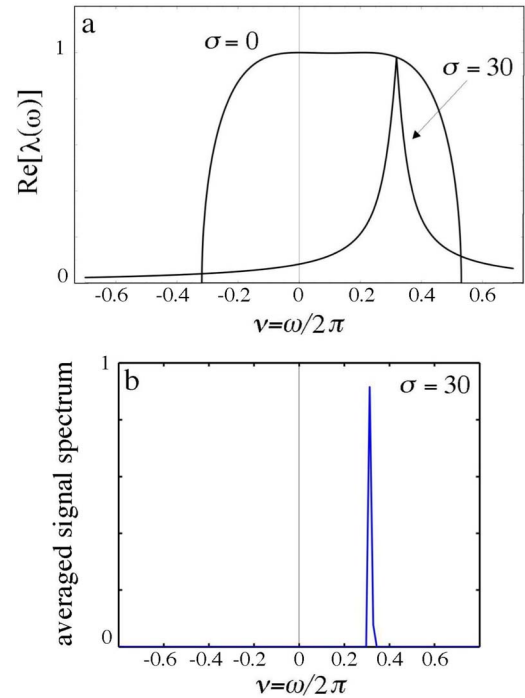


FIG. 5. (Color online) (a) Theoretical spectral gain curve $\operatorname{Re}[\lambda(\omega)]$ of the signal wave in the presence of convection ($\rho_2=0.4, \rho_1=0$), under coherent ($\sigma=0$) and incoherent ($\sigma=30$) excitation [from Eq. (12)]. (b) Numerical simulations of Eqs. (1)–(3) showing the averaged spectrum of the signal wave $\langle |\tilde{A}_1|^2(z_0, \omega) \rangle$ at the propagation distance $z_0=10$. The spectral filtering process induced by dispersion persists in the presence of convection. Note that the simulations confirm the spectral shift of the signal induced by pump incoherence. An average over 15 numerical simulations has been taken to obtain the signal spectrum shown in (b). Parameters are $\beta_3=\beta_2=0.1, \beta_1=0.2$.

the degenerate configuration of the parametric interaction [24]. We have thus shown that this intriguing result may also take place in the nondegenerate configuration, provided that the dispersion parameter of the pump matches the dispersion parameter of one of the daughter waves (Figs. 3 and 4). However, we will show in this section that, in contrast with the degenerate case where both the pump and signal waves evolve towards a coherent state, in the nondegenerate case the system evolves towards a mixed regime of coherent-incoherent interaction.

This mixed regime of interaction is illustrated in Fig. 6, that shows a typical evolution of the spectra of the fields in the incoherent regime of interaction ($L_d/L_{nl} \ll 1$). The incoherent pump amplifies the signal and idler waves from noise fluctuations at the entry of the nonlinear medium $z=0$ (first row of Fig. 6). As described by the gain curve (17), the signal wave rapidly evolves towards a highly coherent state (Fig. 6, second row, $z=2$). Conversely, the idler wave remains incoherent, and quite remarkably, its spectrum tends to duplicate the spectrum of the pump wave, as illustrated in Fig. 6 (third and fourth row, $z=9$). This indicates that the pump and idler waves tend to become mutually coherent during the process of parametric generation, so that their random phases result to be locked with each other. In this

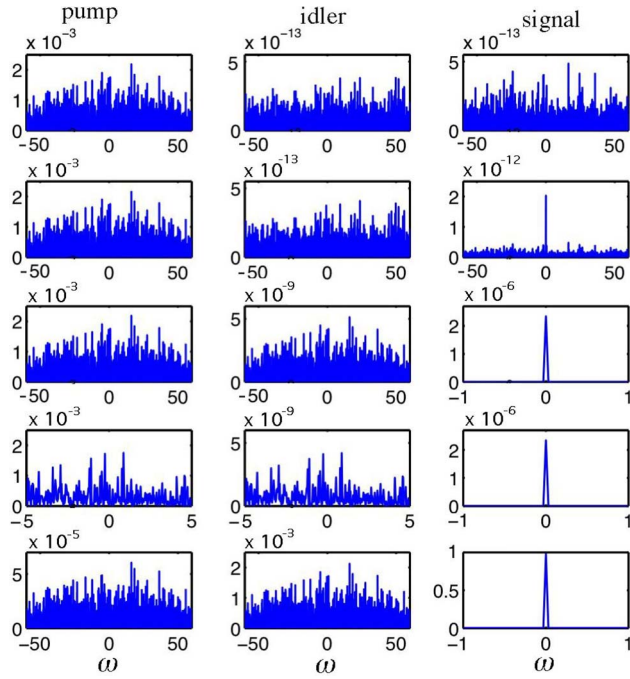


FIG. 6. (Color online) Numerical simulation of Eqs. (1)–(3) (without convection $\rho_1 = \rho_2 = 0$) that illustrates the evolution of the spectra of the three waves during the propagation. This simulation shows the formation of the mixed regime of coherent-incoherent interaction. The incoherent pump amplifies the signal and idler waves from small amplitude noise fluctuations (first row, $z=0$). The signal evolves towards a coherent state (second row, $z=2$). The idler spectrum evolves towards the pump spectrum (third row, $z=9$), as illustrated through a zoom of the frequency window in the fourth row ($z=9$). The mixed regime of coherent-incoherent interaction persists in the presence of significant pump depletion (fifth row, $z=16$). Parameters are $\beta_1=0.2, \beta_2=\beta_3=0.1, \sigma=80$.

way, the idler phase cancels the fast phase fluctuations of the pump wave, which in turn allows the signal to evolve towards a coherent state. This section is devoted to demonstrate this result rigorously by calculating the degree of mutual coherence between the incoherent pump and the incoherent idler waves during their propagation in the nonlinear medium.

A. Pump-idler correlation function

We calculate the degree of mutual coherence between the pump and idler waves during their linear regime of parametric interaction,

$$\mu_{2,3}(z) = \frac{|\Lambda_0(z)|}{\sqrt{\langle |A_3(z,t)|^2 \rangle \langle |A_2(z,t)|^2 \rangle}}, \quad (18)$$

where $\Lambda_0(z) = \langle A_3(z,t) A_2^*(z,t) \rangle$ is the mutual coherence function. For the sake of simplicity and clarity, we assume that the influence of convection between the interacting waves may be neglected, i.e., $L_{cv}/L_{nl} \gg 1$, $L_{cv}/L_d \gg 1$. Writing Eqs. (1)–(3) in Fourier space, and exploiting the formal solution of the signal wave

$$\begin{aligned} \tilde{A}_1(z, \omega) &= (i/2\pi) \int_0^z dz' \int d\omega_1 \exp[-i\beta_1 \omega^2(z-z')] \\ &\quad \times A_3(z', \omega_1) A_2^*(z', \omega_1 - \omega), \end{aligned}$$

one readily obtains the following equation for the evolution of the pump-idler correlator $J_2 = \langle \tilde{A}_3(z, \omega_0) \tilde{A}_2^*(z, \omega) \rangle$:

$$\begin{aligned} \frac{\partial}{\partial z} J_2 &= i(\beta_2 \omega^2 - \beta_3 \omega_0^2) J_2 + \frac{1}{(2\pi)^4} \int \int_{\mathbb{R}^2} d\omega_1 d\omega_2 \\ &\quad \times \int_0^z dz' \exp[-i\beta_1(\omega_2 - \omega)^2(z-z')] J_4, \quad (19) \end{aligned}$$

where J_4 represents the following fourth-order correlator,

$$J_4 = \langle \tilde{A}_3(z, \omega_0) \tilde{A}_3^*(z, \omega_2) \tilde{A}_3(z', \omega_1) \tilde{A}_2^*(z', \omega_1 - \omega_2 + \omega) \rangle.$$

Let us recall that the pump and idler waves are assumed to obey a stationary statistics, so that $J_2 = (2\pi)^2 \tilde{\Lambda}(z, \omega) \delta(\omega - \omega_0)$, where $\tilde{\Lambda}(z, \omega) = \int \Lambda(z, \tau) \exp(-i\omega\tau) d\tau$ is the Fourier transform of the cross-correlation function $\Lambda(z, \tau) = \langle A_3(z, t+\tau) A_2^*(z, t) \rangle$. To get a closed equation for the second-order correlator J_2 , we make use of the property of factorizability of stochastic Gaussian fields. We may thus factorize J_4 as a sum of products of second order correlators,

$$\begin{aligned} \frac{J_4}{(2\pi)^4} &= \Gamma(\omega) \tilde{\Lambda}(z', \omega_1) \delta(\omega_0 - \omega_2) \delta(\omega - \omega_2) + \Gamma(\omega_1) \tilde{\Lambda}(z', \omega) \\ &\quad \times \exp[i\beta_3(\omega_1^2 - \omega^2)(z-z')] \delta(\omega_2 - \omega_1) \delta(\omega - \omega_0), \end{aligned}$$

where we exploited the linear dispersive evolution of the Fourier-pump components $\tilde{A}_3(z, \omega) = \tilde{A}_3(z', \omega) \exp[-i\beta_3 \omega^2(z-z')]$. We substitute the expansion of J_4 into Eq. (19), which gives the following equation governing the evolution of the cross-spectral function,

$$\frac{\partial}{\partial z} \tilde{\Lambda}(z, \omega) = i\epsilon \omega^2 \tilde{\Lambda}(z, \omega) + \Gamma(\omega) \int_0^z dz' \int d\omega_1 \tilde{\Lambda}(z', \omega_1) + \Theta, \quad (20)$$

where $\epsilon = \beta_2 - \beta_3$, and

$$\Theta = \int_0^z \tilde{\Lambda}(z', \omega) \exp[i\varphi_\omega(z-z')] dz', \quad (21)$$

with $\varphi_\omega = -(\beta_1 + \beta_3)\omega^2 + (\beta_1 - \beta_3)\sigma^2 + 2i\beta_1\omega\sigma$. This expression of Θ has been obtained by calculating the integral over ω_1 in (19) by the method of residues [$\Gamma(\omega_1) = \sigma / [\pi(\sigma^2 + \omega_1^2)]$].

Let us study the evolution of the cross-spectral function $\tilde{\Lambda}(z, \omega)$ [Eq. (20)] through the analysis of the growth-rate γ , of the cross correlation between the pump and idler fields. For this purpose, we apply the Laplace transform to Eq. (20), $\hat{\Lambda}(\gamma, \omega) = \int_0^z \tilde{\Lambda}(z, \omega) \exp(-\gamma z) dz$, which allows us to derive the following expression for the cross-correlation growth-rate γ ,

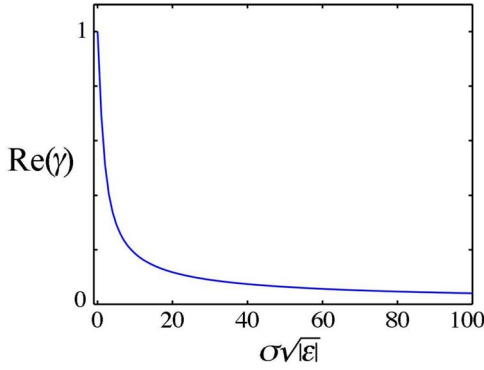


FIG. 7. (Color online) Influence of the mismatch between the pump and idler dispersion ($\epsilon = \beta_3 - \beta_2$) on the growth rate γ of their correlation function during the parametric amplification process. When $\sigma\sqrt{|\epsilon|} \ll 1$, the incoherent idler wave becomes mutually coherent to the incoherent pump wave.

$$\gamma = \int_{-\infty}^{+\infty} \frac{\Gamma(\omega)}{\gamma - i\epsilon\omega^2 - \frac{1}{\gamma - i\varphi_\omega}} d\omega. \quad (22)$$

Note that the last term in the denominator, $1/(\gamma - i\varphi_\omega)$, comes from the function Θ in Eq. (20). In the Appendix we show that this term has a negligible contribution to the growth-rate γ provided that (i) $\beta_1 \neq \beta_3$, (ii) the interaction takes place in the full incoherent regime $L_{d,j}/L_{nl} = 1/\sigma^2|\beta_j| \ll 1$ ($j=1, 3$) (see the Appendix). Neglecting this term, the integral (22) may easily be calculated by the method of residues, which gives $\gamma^2 = 1 - \sigma\sqrt{|\epsilon|}\gamma - i\epsilon\sigma^2\gamma$. The analytical solutions to this algebraic equation are quite involved, and we do not report them explicitly here. We illustrate the physical meaningful solution in Fig. 7, that shows the growth-rate $\text{Re}(\gamma)$ vs the parameter $\sigma\sqrt{|\epsilon|}$. It clearly shows that, regardless of the degree of pump incoherence σ , the growth rate of the correlation between the pump and idler waves is maximum ($\gamma=1$) when the dispersion parameters β_3 and β_2 are matched ($\epsilon=0$). This indicates that in this regime ($\beta_2=\beta_3$), the idler wave adapts its phase to the random phase of the pump wave, as we previously anticipated from the numerical simulations (Fig. 6). Conversely, for a nonvanishing value of ϵ , the correlation growth-rate γ decreases monotonically as the pump becomes incoherent (σ increases). In other terms, the phase-locking between the pump and idler waves becomes less efficient as ϵ , or σ , increase.

As a result, in the full incoherent regime of interaction $L_d/L_{nl} \ll 1$, and in the limit $\beta_1 \neq \beta_2 = \beta_3$, the correlation between the pump and idler waves grows efficiently during their propagation. This result becomes apparent through the analysis of Eq. (20) in the limits $\epsilon=0$, and $\Theta=0$ [i.e., neglecting $1/(\gamma - i\varphi_\omega)$ in Eq. (22), see the Appendix]. In these limits, one may integrate Eq. (20) over ω , to get the following expression for the evolution of the mutual coherence function $\Lambda_0(z) = \Lambda(z, \tau=0) = \langle A_3(t, z) A_2^*(t, z) \rangle = \int \Lambda(z, \omega) d\omega$,

$$d_{zz}\Lambda_0(z) - \Lambda_0(z) = 0. \quad (23)$$

Also note that $d_z\Lambda_0 = \int_0^z \Lambda_0(z') dz'$ from Eq. (20), so that the growth of the mutual coherence occurs with a vanishing

slope at $z=0$, $d_z\Lambda_0|_{z=0}=0$. Accordingly, the mutual coherence function solving (23) reads

$$\Lambda_0(z) = \Lambda_{00} \cosh(z), \quad (24)$$

where $\Lambda_{00} = \langle A_3(z=0, t) A_2^*(z=0, t) \rangle$ corresponds to the initial value of the mutual coherence function.

B. Degree of mutual coherence

To determine the evolution of the degree of mutual coherence between the pump and idler waves we must normalize their mutual coherence function $\Lambda_0(z)$ by their respective average intensities [see Eq. (18)]. For this purpose, we calculate the evolution of the second-order moment $I_2(z) = \langle A_2(z, t) A_2^*(z, t) \rangle$ by following the same procedure as in Sec. IV A. More precisely, under the assumptions $L_{d,j}/L_{nl} = 1/\sigma\beta_j \ll 1$ ($j=1, 2$), and $\beta_2 = \beta_3$, one obtains the following equation governing the evolution of the averaged idler intensity:

$$d_z I_2 = \Lambda_0(z) \int_0^z \Lambda_0(z') dz' + \text{c.c.}, \quad (25)$$

where c.c. denotes the complex conjugate. Exploiting the expression of $\Lambda_0(z)$ given in Eq. (24), one may readily integrate Eq. (25), to get the evolution of the idler intensity, $I_2(z) = I_{2,0} + |\Lambda_{00}|^2 [\cosh(2z) - 1]/2$, where $I_{2,0} = I_2(z=0)$ is the initial intensity noise of the idler wave. In this way, the evolution of the degree of mutual coherence between the pump and idler waves in their linear regime ($\langle |A_3|^2(z, t) \rangle = 1$) of parametric interaction reads

$$\mu_{2,3}(z) = \frac{|\Lambda_{00}| \cosh(z)}{\sqrt{I_{2,0} + \frac{1}{2} |\Lambda_{00}|^2 [\cosh(2z) - 1]}}. \quad (26)$$

We remark that the function $\mu_{2,3}(z)$ exhibits a monotonic growth, and tends asymptotically towards the unity value, $\mu_{2,3} \rightarrow 1$, as illustrated in Fig. 8 (dashed line). This explicitly shows that, owing to their matched dispersion parameters, the pump and idler waves become mutually coherent during their parametric interaction.

We recall that the degree of mutual coherence (26) has been derived under the assumptions that the interaction takes place in the full incoherent regime, $\sigma^2|\beta_j| \gg 1$ (i.e., $L_d/L_{nl} \ll 1$) and in the limit $\beta_1 \neq \beta_2 = \beta_3$. It is interesting to observe that, although $\mu_{2,3}(z)$ does not depend on the dispersion parameters β_j and the degree of pump incoherence σ , $\mu_{2,3}(z)$ describes accurately the evolution of the degree of mutual coherence between the pump and idler waves. This is well illustrated in Figs. 8(a) and 8(b), that show a quantitative agreement of Eq. (26) with the numerical simulations of Eqs. (1)–(3) for a wide range of values of β_j and σ , provided that $L_d/L_{nl} \ll 1$. However, when nonlinear and dispersion effects become of the same order $L_d/L_{nl} \approx 1$, the phase-locking mechanism does not occur efficiently and the emergence of mutual coherence between the pump and idler waves is only partial [Fig. 8(c)].

As previously anticipated through Fig. 6, the strong correlation between the incoherent pump and idler waves allows

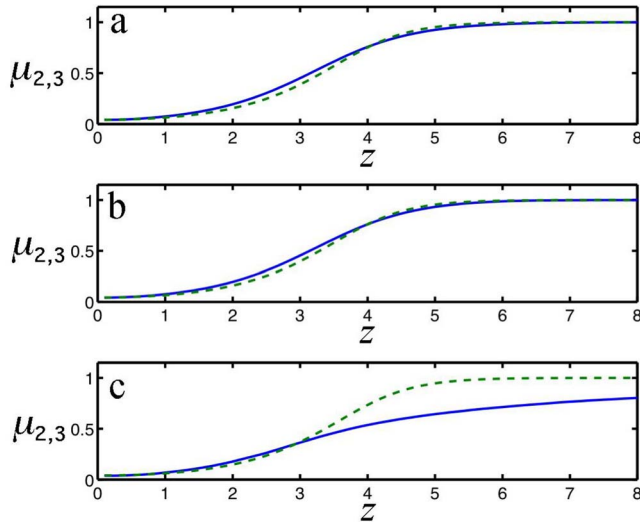


FIG. 8. (Color online) Theoretical [dashed line, from Eq. (26)] and numerical (continuous line) evolution of the degree of mutual coherence between the pump and idler waves during their parametric interaction. When the interaction takes place in the full incoherent regime $L_d/L_{nl} \ll 1$, the idler wave becomes phase correlated to the incoherent pump, $\mu_{2,3} \rightarrow 1$, in agreement with the theory [(a) and (b)]. Conversely, when linear dispersive effects are comparable to nonlinear effects, the phase-locking mechanism is no longer efficient (c). Parameters are (a) $\beta_1=0.2, \beta_2=\beta_3=0.1, \sigma=10^2$, so that $L_d/L_{nl}=10^{-3} \ll 1$, (b) $\beta_1=2 \times 10^{-2}, \beta_2=\beta_3=10^{-2}, \sigma=10^2$, so that $L_d/L_{nl}=10^{-2} \ll 1$, (c) $\beta_1=2 \times 10^{-3}, \beta_2=\beta_3=10^{-3}, \sigma=50$, so that $L_d/L_{nl}=2.5$. The numerical values of $I_{2,0} (=2 \times 10^{-10})$ and $|\Lambda_{00}| (=5.6 \times 10^{-7})$ used to plot Eq. (26) have been determined from the initial random fields generated in the numerical simulations. The simulations have been performed in the absence of convection ($\rho_1=\rho_2=0$). An average over 30 numerical realizations has been taken to obtain the continuous curves (a), (b), (c).

the signal to evolve towards a highly coherent state. As a result, the pump and signal waves should be uncorrelated, a feature which is confirmed by the numerical simulations of Eqs. (1)–(3). Figure 9 illustrates the evolution of the degree of mutual coherence between the pump and signal waves $\mu_{1,3}(z) = |\langle A_3(z,t)A_1^*(z,t) \rangle| / [(\langle |A_3(z,t)|^2 \rangle \langle |A_1(z,t)|^2 \rangle)]^{1/2}$. As expected, the two waves remain uncorrelated during their propagation $\mu_{1,3}(z) < 0.1$, which confirms, *a posteriori*, the assumption employed to factorize the pump-idler correlator [see Eq. (9)].

V. EXPERIMENTAL CONFIGURATION

In order to motivate the experimental confirmation of the process of signal coherence enhancement induced by pump incoherence reported in Sec. III, let us briefly comment the feasibility of such an experiment in noncentrosymmetric optical crystals with quadratic nonlinearity. Thanks to the large variety of nonlinear optical crystals, this system seems to be the most promising. We recall that the experiment aimed at observing the generation of a coherent signal from an incoherent pump imposes severe constraints on the dispersion properties of the three interacting waves. In the following we

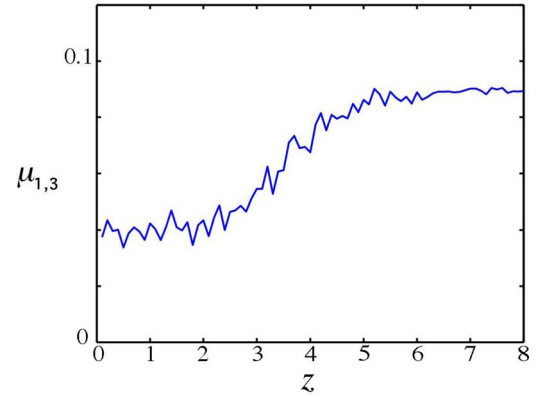


FIG. 9. (Color online) Numerical simulation that shows the evolution of the mutual coherence $\mu_{1,3}(z)$ between the incoherent pump and the generated signal wave during their parametric interaction. As described by the phase-locking mechanism, the signal evolves towards a coherent state which is uncorrelated with the pump wave $\mu_{1,3} < 0.1$. The parameters are the same as in Fig. 8(b) ($\beta_1=2 \times 10^{-2}, \beta_2=\beta_3=10^{-2}, \sigma=10^2, \rho_1=\rho_2=0$). An average over 30 numerical realizations has been taken.

illustrate how the dispersion parameters k_j'' , as well as the group velocities v_j , may easily be tuned by exploiting the dispersion induced by an optical waveguide. Indeed, it is well known that the dispersion properties of a guided wave can be tailored by using an appropriate waveguide index profile. This technique has been proposed, for example, with triply clad (W) fibers to cancel the material dispersion with the waveguide dispersion [29].

In the following we illustrate this technique by considering the concrete example of a lithium niobate (LiNbO₃) channel waveguide. The choice of the LiNbO₃ crystal is motivated by the fact that it is of considerable interest for nonlinear optical application due to its large quadratic nonlinear optical coefficients that can be engineered through the quasispace matched gratings, and the possibility to form low losses optical waveguides by the proton exchange (PE) technique [30]. Which is of main interest for the present purpose concerns the nondegenerate configuration of the parametric interaction and the possibility to match the dispersion parameters of the pump and idler waves ($\beta_2=\beta_3$). It is shown here that this matching can be achieved by using a “mexican-hat” shape of the index profile along the width direction of the waveguide (Fig. 10), and with a classical 3.3 μm Gaussian index profile along the depth direction. From a technological point of view, no major difficulty exists to realize such an index profile, since the waveguide fabrication is based on the well known and widely used PE technique. Nevertheless, two-step fabrication process with appropriate lithographic masks will be necessary to realize the required index profile. The first step will consist of the fabrication of a classical straight waveguide by PE using a single strip of 5 μm aperture mask. Then, a second PE with a double strip mask of 1 μm aperture will create the side lobes of the index profile.

Using the Sellmeier equation [31] for the index substrate, and taking into account the realistic index profile, we calculated the dispersion coefficient k'' , and group velocity $1/v$, as a function of the wavelength λ for the considered waveguide

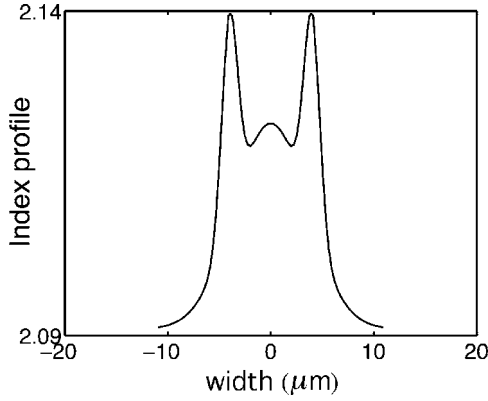
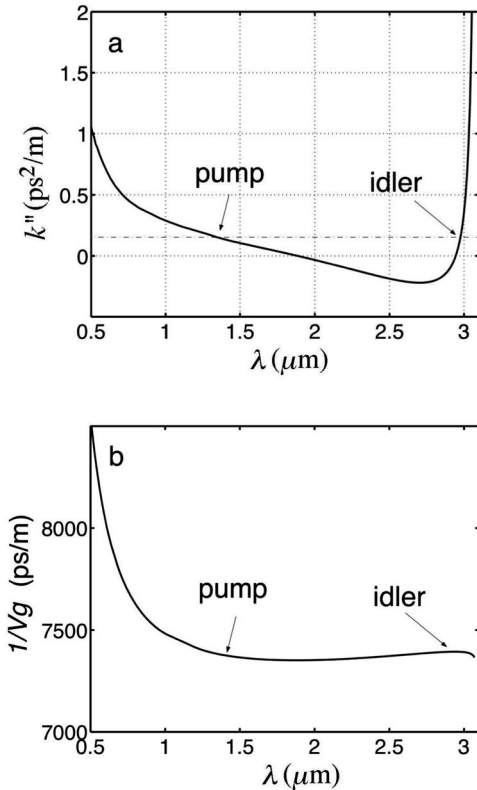
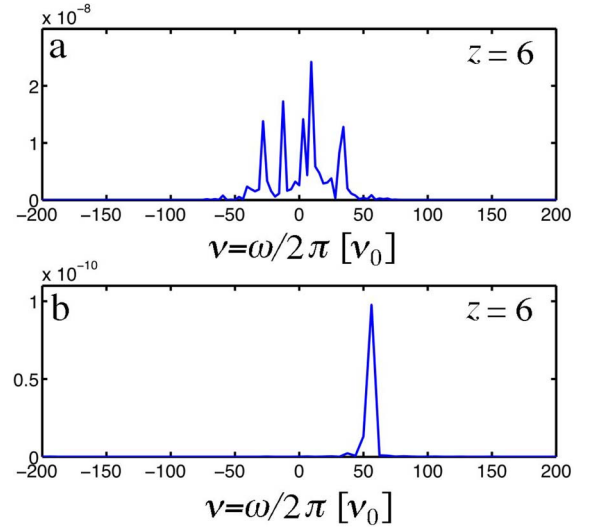


FIG. 10. Waveguide index profile in the width direction.

[see Figs. 11(a) and 11(b)]. One can note the possibility to have ($k_2''=k_3''=0.172$ ps²/m) if pump wavelength is $\lambda_3=1.3$ μm and idler wavelength is $\lambda_2=2.973$ μm . Note that for these wavelengths the velocities of the pump and idler waves are almost matched, $1/v_3-1/v_2\approx-1.7$ m/s, so as to avoid the detrimental influence of convective effects between the two incoherent waves (see Sec. III B). Energy conservation ($\omega_3=\omega_2+\omega_1$) imposes the signal wavelength $\lambda_1=2.31$ μm , so that $k_1''=-0.130$ ps²/m, and $1/v_1=7.32\times 10^3$ ps/m. The quasi-phase-matching condition ($k_3=k_1+k_2+2\pi/\Lambda$) may thus be satisfied with a grating pitch of $\Lambda=26.38$ μm .


FIG. 11. Calculated dispersion coefficient k'' (a) and group-velocity $1/v_g$ (b) as a function of the wavelength λ for the considered quadratic nonlinear optical crystal (see Sec. V).

FIG. 12. (Color online) Numerical simulations showing the spectrum of the signal wave at the propagation distance $z=6L_{nl}$, in the presence of a coherent (a), and incoherent (b), pump. The parameters are determined from the realistic experimental conditions discussed in the text ($v_0=9$ GHz). The incoherent pump leads to a spectral filtering of the generated signal, as described by the theory (Sec. III B). Note also that the incoherent pump induces a spectral shift of the generated signal wave, in agreement with the theoretical expression (12) (see Fig. 5).

As discussed in Secs. III and IV, the phenomenon of coherence enhancement induced by pump incoherence occurs efficiently in the incoherent regime of interaction characterized by $L_d/L_{nl}\ll 1$ [Eq. (6)]. Note that this inequality may be satisfied by decreasing the average intensity of the pump wave $e_0^2=\langle|A_3|^2\rangle$, or its time correlation τ_c . We illustrate in Fig. 12 a typical numerical simulation of Eqs. (1)–(3) implemented with the previously specified parameters. Figure 12 represents the spectrum of the signal wave generated from a coherent (a), and an incoherent pump (b), respectively. In this example we considered a pump wave characterized by an averaged intensity $e_0^2=0.2$ MW/cm², and a spectral width $\Delta\nu=16$ THz ($\tau_c=1/\pi\Delta\nu\approx 20$ fs), so that $L_{d,3}/L_{nl}\approx 0.1$ and $L_{cv,2}/L_{nl}\approx 0.4$. Let us stress that the coherence of the generated signal is approximately two orders of magnitude higher than that of the pump wave [Fig. 12(b)], while the coherence of the idler wave is comparable to the pump wave, in agreement with the theory (Sec. IV). It is important to remark that the coherence acquired by the signal when it is generated from an incoherent pump (b), is higher than that acquired in the presence of a fully coherent pump (a). Finally note that the incoherent pump induces a spectral shift of the generated signal wave, as predicted from the theory (see Fig. 5 in Sec. III B).

VI. CONCLUSION

In summary, we studied the influence of group-velocity dispersion on the coherence properties of the parametric three-wave interaction driven from an incoherent pump wave. We showed the existence of a dispersion-induced

phase-locking mechanism in which the incoherence of the pump may be absorbed by the idler wave, allowing the signal to grow efficiently with a high degree of coherence. More precisely, we showed that owing to their matched dispersion parameters, the incoherent idler wave becomes mutually coherent to the pump during its parametric amplification process. We calculated explicitly the degree of mutual coherence between the incoherent pump and idler waves, and showed that they become fully correlated in the regime of incoherent wave interaction, in complete agreement with the theory. In this way, we generalized the phase-locking mechanism induced by group-velocity difference (convection) between the three waves [20,21]. However, contrary to the convection-induced phase-locking mechanism, we showed that dispersion is responsible for an intriguing spectral filtering process, in which the fluctuations of the incoherent pump appear as having a filtering action on the spectral gain curve of the signal wave. It turns out that the coherence acquired by the signal in the presence of an incoherent pump, is higher than that acquired in the presence of a fully coherent pump. To motivate the experimental study of this phenomenon in the context of nonlinear optics, we characterized the dispersion properties of an actual quadratic nonlinear crystal in its guided-wave configuration. According to this preliminary theoretical study, we may expect to observe the process of coherence enhancement induced by pump noise fluctuations in a near future, thanks to currently available nonlinear optical crystals.

Let us emphasize that the mixed regime of coherent-incoherent interaction induced by dispersion could not be described by the usual kinetic theory of the incoherent three-wave interaction, because the random phase approximation approach implicitly assumes the interacting fields to be incoherent, as well as mutually incoherent [2,5,6,13]. It would be interesting to extend the kinetic wave theory by taking into account phase-correlations effects between the incoherent fields. This important issue is presently under investigation.

Although we restricted our theory to the three-wave interaction in quadratic nonlinear media, it may easily be extended to the four-wave interaction in cubic nonlinear media. Beside the context of optics, the present work is also relevant to many branches of nonlinear wave physics, owing to the universality of the parametric wave mixing process. For instance, our results are of potential interest to the area of finite

temperature atomic-molecular Bose-Einstein condensates [32], which may be described classically in terms of incoherent matter waves [33]. More generally, the experimental verifications of our predictions would be of interest for the fundamental study of self-organization processes in nonlinear stochastic environments [34], such as, e.g., the recently studied systems of incoherent solitons in inertial nonlinear media [9,35].

APPENDIX

In the strong incoherent regime of interaction, $\sigma\beta_j^2 \gg 1$ ($j=1, 2, 3$), i.e., $L_{d,j}/L_{nl} \ll 1$, we may assume $|\varphi_\omega| \gg 1$ if $\beta_1 \neq \beta_3$. This allows us to treat perturbatively the last term in the denominator of Eq. (22), i.e., $1/(\gamma - i\varphi_\omega)$. Accordingly, the integral equation for the cross-correlation growth-rate (22) takes the simplified form

$$\gamma^2 = 1 - \frac{i}{\gamma} K, \quad (\text{A1})$$

$$K = \int_{-\infty}^{+\infty} \frac{\Gamma(\omega)}{\varphi_\omega} d\omega, \quad (\text{A2})$$

where we have implicitly assumed that $\beta_1 \neq \beta_2 = \beta_3$, so as to take advantage of the dispersion-induced phase-locking mechanism between A_2 and A_3 . Assuming the spectrum of the pump to be Lorentzian, the integral (A2) may easily be calculated by the method of the residues, which gives

$$K = \frac{1}{4\beta_1\sigma^2} \quad \text{for} \quad \frac{\beta_1 - \beta_3}{\beta_1 + \beta_3} > 0$$

and

$$K = \frac{1}{4\beta_1\sigma^2} - \frac{1}{\beta_1\sigma^2 \left(\frac{\beta_1 - \beta_3}{\beta_1 + \beta_3} - 1 \right)^2} \quad \text{for} \quad \frac{\beta_1 - \beta_3}{\beta_1 + \beta_3} < 0.$$

It results that in the limit $\sigma\beta_j^2 \gg 1$ ($j=1, 2$), the integral K in (A1) has a negligible contribution, $|K| \ll 1$, so that the cross-correlation growth rate given in (A1) reduces to $\gamma = \pm 1$, in agreement with Eq. (23) that governs the evolution of the mutual coherence function.

-
- [1] R. Z. Sagdeev, D. A. Usikov, and G. M. Zaslavsky, *Nonlinear Physics* (Harwood, New York, 1988).
 [2] V. E. Zakharov, V. S. L'vov, and G. Falkovich, *Kolmogorov Spectra of Turbulence I* (Springer, Berlin, 1992).
 [3] A. D. D. Craik, *Wave Interactions and Fluid Flows* (Cambridge University Press, Cambridge, 1985); E. Infeld and G. Rowlands, *Nonlinear Waves, Solitons and Chaos* (Cambridge University Press, Cambridge, 1992).
 [4] M. F. Hamilton and D. T. Blackstock, *Nonlinear Acoustics* (Academic, New York, 1998), Chap. 8, p. 14.
 [5] V. N. Tsytovich, *Nonlinear Effects in Plasma* (Plenum, New

York, 1970).

- [6] A. Hasegawa, *Plasma Instabilities and Nonlinear Effects* (Springer-Verlag, New York, 1975).
 [7] P. A. Robinson, *Rev. Mod. Phys.* **69**, 507 (1997).
 [8] A. C. Newell and J. V. Moloney, *Nonlinear Optics* (Addison-Wesley, New York, 1992); R. W. Boyd, *Nonlinear Optics* (Academic, San Diego, 1992).
 [9] Y. S. Kivshar and G. P. Agrawal, *Optical Solitons : From Fibers to Photonic Crystals* (Academic, New York, 2003).
 [10] *Spatial Solitons*, edited by S. Trillo and W. Torruellas (Springer-Verlag, Berlin, 2001).

- [11] P. Meystre, *Atom Optics* (Springer, New York, 2001); C. J. Pethick and H. Smith, *Bose-Einstein Condensation in Dilute Gases* (Cambridge University Press, Cambridge, 2001).
- [12] P. A. Robinson and P. M. Drysdale, *Phys. Rev. Lett.* **77**, 2698 (1996).
- [13] G. Laval *et al.*, *Phys. Fluids* **20**, 2049 (1977); E. A. Williams *et al.*, *ibid.* **22**, 139 (1979); A. M. Martins and J. T. Mendonça, *Phys. Rev. A* **31**, 3898 (1985); *Phys. Fluids* **31**, 3286 (1988); R. L. Berger, *Phys. Rev. Lett.* **65**, 1207 (1990).
- [14] D. J. Kaup, A. Reiman, and A. Bers, *Rev. Mod. Phys.* **51**, 275 (1979).
- [15] S. C. Chiu, *J. Math. Phys.* **19**, 168 (1978); K. Nozaki and T. Taniuti, *J. Phys. Soc. Jpn.* **34**, 796 (1973); K. Druhl, R. G. Wenzel, and J. L. Carlsten, *Phys. Rev. Lett.* **51**, 1171 (1983); E. Picholle, C. Montes, C. Leycuras, O. Legrand, and J. Botineau, *ibid.* **66**, 1454 (1991); S. F. Morozov *et al.*, *Sov. J. Quantum Electron.* **8**, 576 (1978); A. D. D. Craik *et al.*, *Wave Motion* **15**, 173 (1992); S. Trillo, *Opt. Lett.* **21**, 1111 (1996); C. Montes, A. Mikhailov, A. Picozzi, and F. Ginovart, *Phys. Rev. E* **55**, 1086 (1997); C. Montes, A. Picozzi, and D. Bahloul, *ibid.* **55**, 1092 (1997); A. Picozzi and M. Haelterman, *Opt. Lett.* **23**, 1808 (1998); *Europhys. Lett.* **45**, 463 (1999); *Phys. Rev. E* **59**, 3749 (1999); *Phys. Rev. Lett.* **84**, 5760 (2000); A. Picozzi, *Phys. Rev. E* **64**, 016614 (2001).
- [16] M. J. Werner and P. D. Drummond, *J. Opt. Soc. Am. B* **10**, 2390 (1993); D. E. Pelinovsky, A. V. Buryak, and Y. S. Kivshar, *Phys. Rev. Lett.* **75**, 591 (1995); R. A. Fuerst, D. M. Baboiu, B. Lawrence, W. E. Torruellas, G. I. Stegeman, S. Trillo, and S. Wabnitz, *ibid.* **78**, 2756 (1997); L. Torner, D. Mazilu, and D. Mihalache, *ibid.* **77**, 2455 (1996).
- [17] A. V. Buryak, P. Di Trapani, D. Skryabin, and S. Trillo, *Phys. Rep.* **370**, 63 (2002).
- [18] See, e.g., H. Baldis and C. Labaune, *Plasma Phys. Controlled Fusion* **39**, 51 (1997); J. Fuchs, C. Labaune, H. Bandulet, P. Michel, S. Depierreux, and H. A. Baldis, *Phys. Rev. Lett.* **88**, 195003 (2002).
- [19] A. T. Georges, *Phys. Rev. A* **39**, 1876 (1989); **41**, 388 (1990).
- [20] A. Picozzi and M. Haelterman, *Phys. Rev. Lett.* **86**, 2010 (2001).
- [21] A. Picozzi, C. Montes, and M. Haelterman, *Phys. Rev. E* **66**, 056605 (2002).
- [22] C. Montes, A. Picozzi, and K. Gallo, *Opt. Commun.* **237**, 437 (2004).
- [23] A. Picozzi, M. Haelterman, S. Pitois, and G. Millot, *Phys. Rev. Lett.* **92**, 143906 (2004).
- [24] A. Picozzi and M. Haelterman, *Phys. Rev. Lett.* **92**, 103901 (2004).
- [25] A. Piskarskas, V. Smilgevicius, and A. Stabinis, *Opt. Commun.* **143**, 97 (1997); A. Piskarskas, V. Smilgevicius, A. Stabinis, and V. Vaicaitis, *J. Opt. Soc. Am. B* **16**, 1566 (1999).
- [26] A. Papoulis, *Probability, Random Variables, and Stochastic Processes* (McGraw-Hill, New York, 1965), Chap. 14.
- [27] R. L. Byer and S. E. Harris, *Phys. Rev.* **168**, 1064 (1968); A. Sukhorukov and A. K. Shchednova, *Sov. Phys. JETP* **33**, 677 (1971); J. E. Pearson, A. Yariv, and U. Ganiel, *Appl. Opt.* **12**, 1165 (1973).
- [28] A. Picozzi and M. Haelterman, *Phys. Rev. Lett.* **88**, 083901 (2002); *Phys. Rev. E* **63**, 056611 (2001).
- [29] M. Monerie, *IEEE J. Quantum Electron.* **18**, 535 (1982); T. Miya, K. Okamoto, Y. Ohmori, and Y. Sasaki, *IEEE J. Quantum Electron.* **17**, 858 (1981).
- [30] Hui Zhang, Ming Ju Li, S. Iraj Najafi, and Otto Schwelb, *Appl. Opt.* **33**, 3391, (1994); Yu. N. Korkishko and V. A. Fedorov, *Ion Exchange in Single Crystals for Integrated Optics and Optoelectronics* (Cambridge International Science, Cambridge, UK, 1999).
- [31] V. G. Dmitriev, G. G. Gurzadyan, and D. N. Nikogosyan, *Handbook of Nonlinear Optical Crystals* (Springer-Verlag, Berlin, 1990).
- [32] P. D. Drummond, K. V. Kheruntsyan, and H. He, *Phys. Rev. Lett.* **81**, 3055 (1998); D. J. Heinzen, R. Wynar, P. D. Drummond, and K. V. Kheruntsyan, *ibid.* **84**, 5029 (2000); E. Donley *et al.*, *Nature (London)* **417**, 529 (2002); M. W. Zwiernik, C. A. Stan, C. H. Schunck, S. M. F. Raupach, S. Gupta, Z. Hadzibabic, and W. Ketterle, *Phys. Rev. Lett.* **91**, 250401 (2003).
- [33] See, e.g., Yu. Kagan and B. V. Svistunov, *Phys. Rev. Lett.* **79**, 3331 (1997); M. J. Davis, S. A. Morgan, and K. Burnett, *ibid.* **87**, 160402 (2001); *Phys. Rev. A* **66**, 053618 (2002).
- [34] S. Dyachenko *et al.*, *Zh. Eksp. Teor. Fiz.* **96**, 2026 (1989) [*Sov. Phys. JETP* **69**, 1144 (1989)]; Y. Pomeau, *Physica D* **61**, 227 (1992); S. Dyachenko, A. C. Newell, A. Pushkarev, and V. E. Zakharov, *ibid.* **57**, 96 (1992); R. Jordan, B. Turkington, and C. L. Zirbel, *ibid.* **137**, 353 (2000); R. Jordan and C. Josserand, *Phys. Rev. E* **61**, 1527 (2000); K. Rasmussen, T. Cretegy, P. G. Kevrekidis, and N. Gronbech-Jensen, *Phys. Rev. Lett.* **84**, 3740 (2000); B. Rumpf and A. C. Newell, *ibid.* **87**, 054102 (2001); *Physica D* **184**, 162 (2003).
- [35] M. Mitchell and M. Segev, *Nature (London)* **387**, 880 (1997); D. N. Christodoulides, T. H. Coskun, M. Mitchell, and M. Segev, *Phys. Rev. Lett.* **78**, 646 (1997); M. Mitchell, M. Segev, T. H. Coskun, and D. N. Christodoulides, *ibid.* **79**, 4990 (1997); Z. Chen *et al.*, *Science* **280**, 889 (1998); D. N. Christodoulides, T. H. Coskun, M. Mitchell, Z. Chen, and M. Segev, *Phys. Rev. Lett.* **80**, 5113 (1998); D. N. Christodoulides, E. D. Eugenieva, T. H. Coskun, M. Segev, and M. Mitchell, *Phys. Rev. E* **63**, 035601(R) (2001); B. Hall, M. Lisak, D. Anderson, R. Fedele, and V. E. Semenov, *ibid.* **65**, 035602(R) (2002).